


 Cite this: *RSC Adv.*, 2023, 13, 3295

Quantitative evaluation of the actual hydrogen atom donating activities of O–H bonds in phenols: structure–activity relationship†

 Yan-Hua Fu,^a Yanwei Zhang,^a Fang Wang,^a Ling Zhao,^a Guang-Bin Shen^b and Xiao-Qing Zhu^c

The H-donating activity of phenol and the H-abstraction activity of phenol radicals have been extensively studied. In this article, the second-order rate constants of 25 hydrogen atom transfer (HAT) reactions between phenols and PINO and DPPH radicals in acetonitrile at 298 K were studied. Thermo-kinetic parameters $\Delta G^{\ddagger\circ}(\text{XH})$ were obtained using a kinetic equation [$\Delta G_{\text{XH}/\text{Y}}^{\ddagger} = \Delta G^{\ddagger\circ}(\text{XH}) + \Delta G^{\ddagger\circ}(\text{Y})$]. Bond dissociation free energies $\Delta G^{\circ}(\text{XH})$ were calculated by the iBonD HM method, whose details are available at https://pka.luozsgroup.com/bde_prediction. Intrinsic resistance energies $\Delta G_{\text{XH}/\text{X}}^{\ddagger}$ and $\Delta G^{\ddagger\circ}(\text{X})$ were determined as $\Delta G^{\ddagger\circ}(\text{XH})$ and $\Delta G^{\circ}(\text{XH})$ were available. $\Delta G^{\circ}(\text{XH})$, $\Delta G_{\text{XH}/\text{X}}^{\ddagger}$, $\Delta G^{\ddagger\circ}(\text{XH})$ and $\Delta G^{\ddagger\circ}(\text{X})$ were used to assess the H-donating abilities of the studied phenols and the H-abstraction abilities of phenol radicals in thermodynamics, kinetics and actual HAT reactions. The effect of structures on these four parameters was discussed. The reliabilities of $\Delta G^{\ddagger\circ}(\text{XH})$ and $\Delta G^{\ddagger\circ}(\text{X})$ were examined. The difference between the method of determining $\Delta G_{\text{XH}/\text{X}}^{\ddagger}$ mentioned in this study and the dynamic nuclear magnetic method mentioned in the literature was studied. *Via* this study, not only $\Delta G^{\circ}(\text{XH})$, $\Delta G_{\text{XH}/\text{X}}^{\ddagger}$, $\Delta G^{\ddagger\circ}(\text{XH})$ and $\Delta G^{\ddagger\circ}(\text{X})$ of phenols could be quantitatively evaluated, but also the structure–activity relationship of phenols is clearly demonstrated. Moreover, it lays the foundation for designing and synthesizing more antioxidants and radicals.

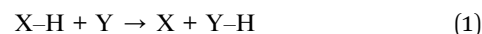
 Received 31st October 2022
 Accepted 31st December 2022

DOI: 10.1039/d2ra06877j

rsc.li/rsc-advances

Introduction

Hydrogen atom transfer (HAT) reactions (eqn (1)) play important roles in a variety of chemical and biological processes and are therefore actively investigated.^{1–3} Research on HAT from a wide variety of substrates, XH (1,4-dihydropyridine,^{4,5} alkanes,⁶ amines and amides,^{7,8} and phenols^{9,10}), by a number of radicals, Y (*N*-oxyl radicals,¹⁰ *C*-oxyl radicals,¹¹ and 2,2-diphenyl-1-picrylhydrazyl (DPPH[•])¹²), has drawn intense attention from chemists. In particular, phenols can not only act as hydrogen atom donors (H-donors) in HAT reactions with free radicals⁹ but also act as hydrogen atom acceptors (H-acceptors) to oxidize many antioxidants¹³ such as 5,6-isopropylidene ascorbate (iAscH^{•-}).¹⁴



In this article, the HAT reaction between 25 phenols XH and phthalimide-*N*-oxyl radical (PINO[•]) and DPPH[•] was researched; parent structures and marks of phenols and radicals examined in this work are shown in Scheme 1. The time-resolved kinetic studies in CH₃CN of the HAT reactions of activated phenols including natural phenols (2,6-dimethyl-, 2,6-di-*tert*-butyl-4-substituted^{15,16} and 4-substituted phenols)¹⁷ (1H–18H), hydrogen-bonded phenols¹⁸ (19H–23H) including (+)-catechin (22H) and caffeic acid (23H), 2,2,5,7,8-pentamethylchroman-6-ol (PMC, 24H)¹⁶ and α -tocopherol (α -TocOH, 25H)¹⁹ with radicals were carried out.

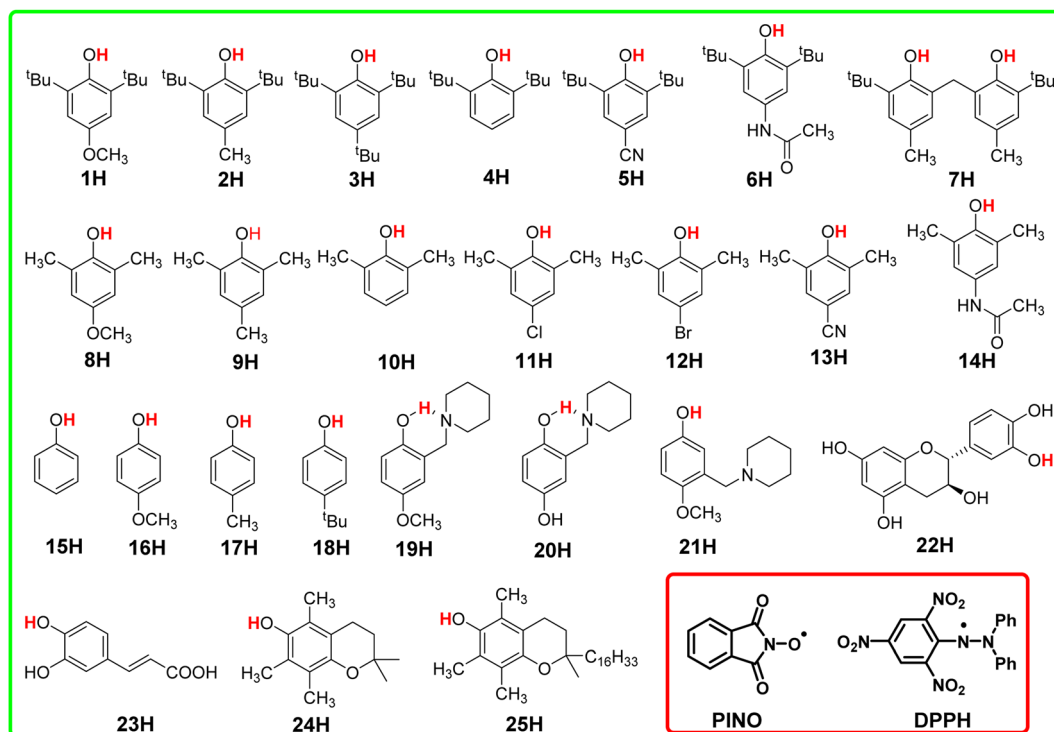
In previous works,^{8,20–24} four physical parameters of H-donor XH, bond dissociation free energy $\Delta G^{\circ}(\text{XH})$, kinetic intrinsic resistance energy $\Delta G_{\text{XH}/\text{X}}^{\ddagger}$, thermo-kinetic parameter $\Delta G^{\ddagger\circ}(\text{XH})$ and $\Delta G^{\ddagger\circ}(\text{X})$, have been used to evaluate the H-donating and H-abstraction activities of XH and the corresponding radical X in thermodynamics, kinetics and actual HAT reactions, respectively. $\Delta G^{\circ}(\text{XH})$ is the thermodynamic factor and usually used to assess the potential H-donating capacity of XH and H-abstraction capacity of X. $\Delta G_{\text{XH}/\text{X}}^{\ddagger}$ is the activation free energy of the self-exchange HAT reaction for XH ($\text{XH} + \text{X} \rightarrow \text{X} + \text{XH}$). It is the kinetic resistance of the HAT reaction as the thermodynamic driving force is zero, which means the kinetic intrinsic

^aCollege of Chemistry and Environmental Engineering, Anyang Institute of Technology, Anyang, Henan, 455000, China. E-mail: 20180031@ayit.edu.cn

^bSchool of Medical Engineering, Jining Medical University, Jining, Shandong, 272000, P. R. China

^cDepartment of Chemistry, Nankai University, Tianjin, 300071, China

 † Electronic supplementary information (ESI) available: The second-order rate constants k_2 and activation free energies $\Delta G_{\text{XH}/\text{Y}}^{\ddagger}$ of HAT reactions from phenols to radicals in acetonitrile at 298 K, and the $\Delta G^{\circ}(\text{XH})$ values determined by theoretical calculation in this work are shown. See DOI: <https://doi.org/10.1039/d2ra06877j>

Scheme 1 Parent structures and marks of phenols and radicals examined in this work.

resistance barrier of XH in HAT reaction. It is also called intrinsic resistance energy. The thermo-kinetic parameter $\Delta G^{\ddagger 0}$ is proposed by a new kinetic model in previous works^{25,26} and consists of both the thermodynamic force and kinetic intrinsic barrier and can be used not only to describe the actual H-donating ability of XH and the H-abstraction ability of X in a chemical reaction during a certain reaction time but also to predict the rate of the HAT reaction (eqn (1)) by kinetic eqn (2). The definitions of $\Delta G^{\ddagger 0}$ are listed in eqn (3) and (4). In this work, $\Delta G^{\circ}(\text{XH})$, $\Delta G_{\text{XH/X}}^{\ddagger}$, $\Delta G^{\ddagger 0}(\text{XH})$ and $\Delta G^{\ddagger 0}(\text{X})$ were investigated to study the H-donating abilities of phenols XH in Scheme 1 and the H-abstraction abilities of the corresponding phenol radicals X.

$$\Delta G_{\text{XH/Y}}^{\ddagger} = \Delta G^{\ddagger 0}(\text{XH}) + \Delta G^{\ddagger 0}(\text{Y}) \quad (2)$$

$$\Delta G^{\ddagger 0}(\text{XH}) \equiv 1/2[\Delta G_{\text{XH/X}}^{\ddagger} + \Delta G^{\circ}(\text{XH})] \quad (3)$$

$$\Delta G^{\ddagger 0}(\text{Y}) \equiv 1/2[\Delta G_{\text{YH/Y}}^{\ddagger} - \Delta G^{\circ}(\text{YH})] \quad (4)$$

Results and discussion

Determination of the “ $\Delta G^{\circ}(\text{XH})$, $\Delta G_{\text{XH/X}}^{\ddagger}$, $\Delta G^{\ddagger 0}(\text{XH})$, and $\Delta G^{\ddagger 0}(\text{X})$ ” values of phenols XH and phenol radicals X

The kinetic studies of the HAT reactions from O–H bonds of phenols to the PINO and DPPH radicals are listed in ESI.†^{15–19,27} The second-order rate constants k_2 and activation free energies $\Delta G_{\text{XH/Y}}^{\ddagger}$ of HAT reactions, which were obtained using the Eyring

equation [$k_2 = (k_{\text{B}}T/h)\exp(-\Delta G^{\ddagger}/RT)$], are listed in Table S1.† As the thermo-kinetic parameters of the PINO radical [$\Delta G^{\ddagger 0}(\text{PINO}) = -34.94 \text{ kcal mol}^{-1}$] and DPPH radical [$\Delta G^{\ddagger 0}(\text{DPPH}) = -29.67 \text{ kcal mol}^{-1}$] were already available in our previous work,²² the thermo-kinetic parameters of phenols $\Delta G^{\ddagger 0}(\text{XH}) = \Delta G_{\text{XH/Y}}^{\ddagger} - \Delta G^{\ddagger 0}(\text{Y})$ can be determined using eqn (2). According to the definition of $\Delta G^{\ddagger 0}(\text{XH})$, as long as the bond dissociation free energies $\Delta G^{\circ}(\text{XH})$ of XH are available, the intrinsic resistance energies $\Delta G_{\text{XH/X}}^{\ddagger}$ can be obtained by eqn (3). In this work, the bond dissociation energies (BDE) of O–H bonds of phenols in acetonitrile were calculated by the iBonD HM method developed by Luo and Zhang in 2020, whose details are available at https://pka.luozsgroup.com/bde_prediction.^{28,29} It is a holistic BDE prediction model (HM) based on the iBonD experimental dataset.³⁰ Many methods such as quantum chemistry (QC), molecular dynamics (MD), and Monte Carlo (MC) simulation methods reported in the literature for the theoretical calculation of BDE were used to calculate the reaction sites and hydrogen dissociation energy of HTPB propellant antioxidants.³¹ The iBonD HM model has provided so far the best accuracy in prediction non-aqueous BDE and is equally applied for aqueous and micro-BDE prediction. $\Delta G^{\circ}(\text{XH})$ can be obtained by subtracting $4.9 \text{ kcal mol}^{-1}$ from the BDE values.³² Subsequently, $\Delta G_{\text{XH/X}}^{\ddagger}$ can be obtained using eqn (3). At the same time, $\Delta G^{\ddagger 0}(\text{X})$ of phenol radicals can be determined as long as $\Delta G_{\text{XH/X}}^{\ddagger}$ and $\Delta G^{\circ}(\text{XH})$ of XH are available according to eqn (4). These four physical parameters of the studied phenols and phenol radicals are listed in Table 1.



Table 1 $\Delta G^\circ(\text{XH})$, $\Delta G_{\text{XH}/\text{X}}^\ddagger$, $\Delta G^{\ddagger\circ}(\text{XH})$, and $\Delta G^{\ddagger\circ}(\text{X})$ of XH in HAT reactions in CH_3CN at 298 K

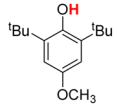
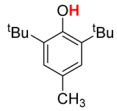
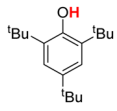
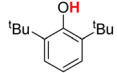
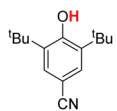
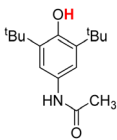
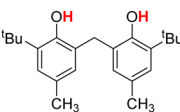
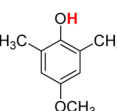
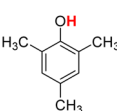
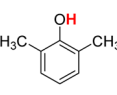
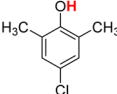
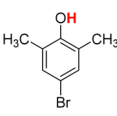
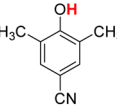
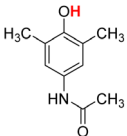
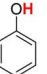
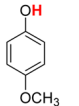
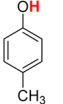
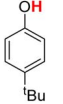
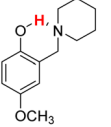
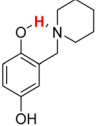
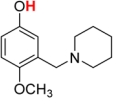
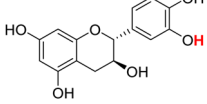
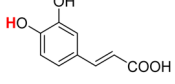
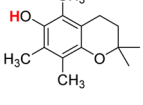
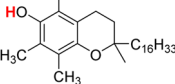
XH	Structure	kcal mol ⁻¹			
		$\Delta G^\circ(\text{XH})^a$	$\Delta G_{\text{XH}/\text{X}}^\ddagger^b$	$\Delta G^{\ddagger\circ}(\text{XH})^c$	$\Delta G^{\ddagger\circ}(\text{X})^d$
1H		72.70	17.88	45.29	-27.41
2H		75.30	18.25	46.78	-28.52
3H		76.70	18.03	47.37	-29.33
4H		78.00	18.11	48.05	-29.95
5H		79.50	18.28	48.89	-30.61
6H		73.30	19.04	46.17	-27.13
7H		76.50	6.34	41.42	-35.08
8H		73.10	13.31	43.20	-29.90
9H		77.20	12.67	44.94	-32.26
10H		79.50	12.98	46.24	-33.26
11H		79.20	17.94	48.57	-30.63
12H		79.00	14.04	46.52	-32.48
13H		79.60	19.97	49.79	-29.81



Table 1 (Contd.)

XH	Structure	kcal mol ⁻¹			
		$\Delta G^{\circ}(\text{XH})^a$	$\Delta G_{\text{XH/X}}^{\ddagger b}$	$\Delta G^{\ddagger 0}(\text{XH})^c$	$\Delta G^{\ddagger 0}(\text{X})^d$
14H		79.40	7.97	43.68	-35.72
15H		81.90	17.03	49.46	-32.44
16H		78.70	13.62	46.16	-32.54
17H		83.00	14.49	48.74	-34.26
18H		81.10	17.14	49.12	-31.98
19H		75.60	10.23	42.92	-32.68
20H		76.20	8.84	42.52	-33.68
21H		75.90	11.66	43.78	-32.12
22H		76.60	14.32	45.46	-31.14
23H		75.20	16.17	45.68	-29.52
24H		72.70	9.17	40.93	-31.77
25H		74.30	12.59	43.45	-30.85

^a $\Delta G^{\circ}(\text{XH})$ values are obtained by the iBond HM method in this work. ^b $\Delta G_{\text{XH/X}}^{\ddagger}$ values are derived from eqn (3). ^c $\Delta G^{\ddagger 0}(\text{XH})$ values are derived from eqn (2). ^d $\Delta G^{\ddagger 0}(\text{X})$ values are derived from eqn (4).



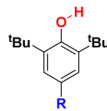
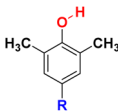
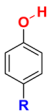
Potential H-donating capacities of phenols $\Delta G^\circ(\text{XH})$

As well known, the bond dissociation free energies $\Delta G^\circ(\text{XH})$ of O–H bonds in phenols are the thermodynamics parameters, and can be used to assess the potential H-donating capacities of O–H bonds with different structures. The bigger the $\Delta G^\circ(\text{XH})$ value is, the weaker the potential H-donating capacity of XH is. In order to discover the relationship of $\Delta G^\circ(\text{XH})$ on the structures of XH, the direct vision dependence of $\Delta G^\circ(\text{XH})$ on the structures of XH is shown in Scheme 2. From Scheme 2, it is clear that the $\Delta G^\circ(\text{XH})$ values of these phenols in CH_3CN at 298 K range from 72.70 kcal mol⁻¹ for PMC (24H) and 2,6-di-*tert*-butyl-4-methoxyphenol (1H) to 83.00 kcal mol⁻¹ for 2-methylphenol (17H), and the structures of XH have great effect on the $\Delta G^\circ(\text{XH})$ values.

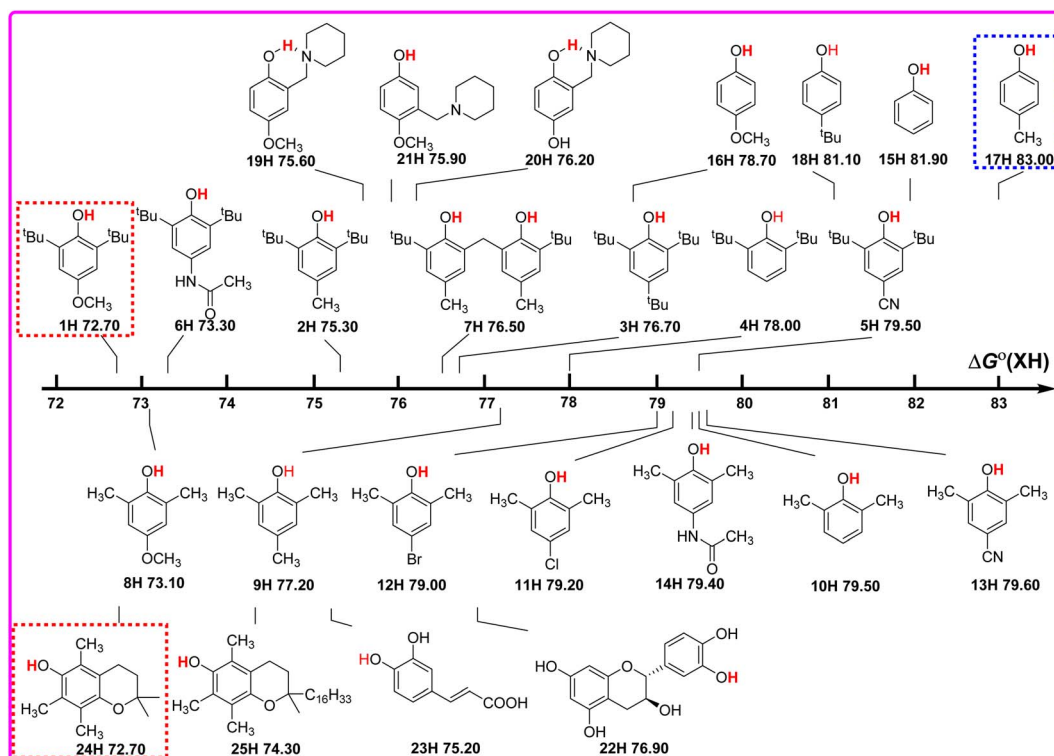
For 2,6-di-*tert*-butylphenol series (1H–7H), 2,6-dimethylphenol series (8H–14H) and 4-substituted phenols (15H–18H), combined with the electronic effect of substituents on $\Delta G^\circ(\text{XH})$, the order of $\Delta G^\circ(\text{XH})$ of three types of phenols is 2,6-di-*tert*-butylphenol series > 2,6-dimethylphenol series > 4-substituted phenols. In the same series, for example, 2,6-di-*tert*-butylphenol series (1H–7H), with the different electronic effects of substituents at position 4, the $\Delta G^\circ(\text{XH})$ values of O–H bonds increase from the electron-donating groups to the electron-withdrawing groups ($\text{OCH}_3 > \text{CH}_3\text{CONH} > \text{CH}_3 > \text{tBu} > \text{H} > \text{CN}$), and the H-donating capacities decrease gradually. In order to obtain the electronic effects of the substituents at position 4, the changes in bond dissociation free energy $\Delta\Delta G^\circ$ between H-substituted phenols (4H, 10H and 15H) and other substituents in the 2,6-di-*tert*-butylphenol series, 2,6-dimethylphenol series

and 4-substituted phenols respectively, are compared in Table 2. As can be seen from Table 2, in these three different phenol series, the $\Delta\Delta G^\circ$ values caused by the electronic effect of the substituent at position 4 are not the same. Therefore, the electronic effect of the substituent at position 4 of phenol cannot be obtained simply by comparing the changes in $\Delta G^\circ(\text{XH})$. Since $\Delta G^\circ(\text{XH})$ represents the homolytic bond dissociation free

Table 2 Energy changes $\Delta\Delta G^\circ$ caused by the introduction of –R substituents at position 4 in 2,6-di-*tert*-butylphenol, 2,6-di-methylphenol series and 4-substituted phenols in CH_3CN at 298 K

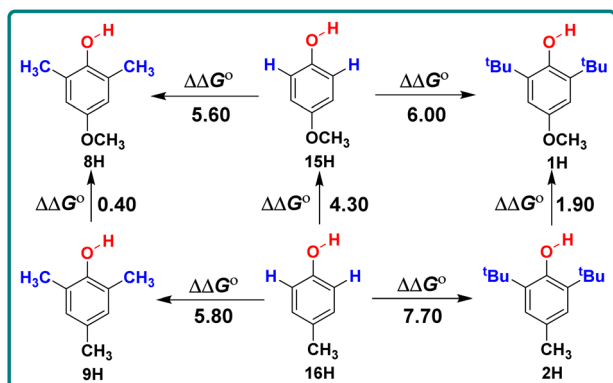
	$\Delta\Delta G^{\circ a}$ (kcal mol ⁻¹)		
			
–R			
OCH_3	5.30	6.40	3.20
CH_3CONH	4.70	0.10	1.00 ^b
CH_3	2.70	2.30	–1.10
<i>t</i> Bu	1.30	0.90 ^b	0.80
H	0.00	0.00	0.00
Cl	0.50 ^b	0.30	–3.50 ^b
Br	1.30 ^b	0.50	–1.80 ^b
CN	–1.50	–0.10	–5.90 ^b

^a $\Delta\Delta G^\circ$ values are given by $\Delta G^\circ(\text{R}=\text{H})$ minus $\Delta G^\circ(\text{R})$. ^b $\Delta G^\circ(\text{XH})$ determined by the iBond HM method in this work are listed in Table S2.



Scheme 2 Visual comparison of $\Delta G^\circ(\text{XH})$ among the 25 phenols of O–H bonds in CH_3CN at 298 K, the unit is kcal mol⁻¹.





Scheme 3 Energy changes $\Delta\Delta G^\circ$ for 2,6-disubstituted-4-methoxyphenol series and 2,6-disubstituted-4-methylphenol in CH_3CN at 298 K, the unit is kcal mol^{-1} .

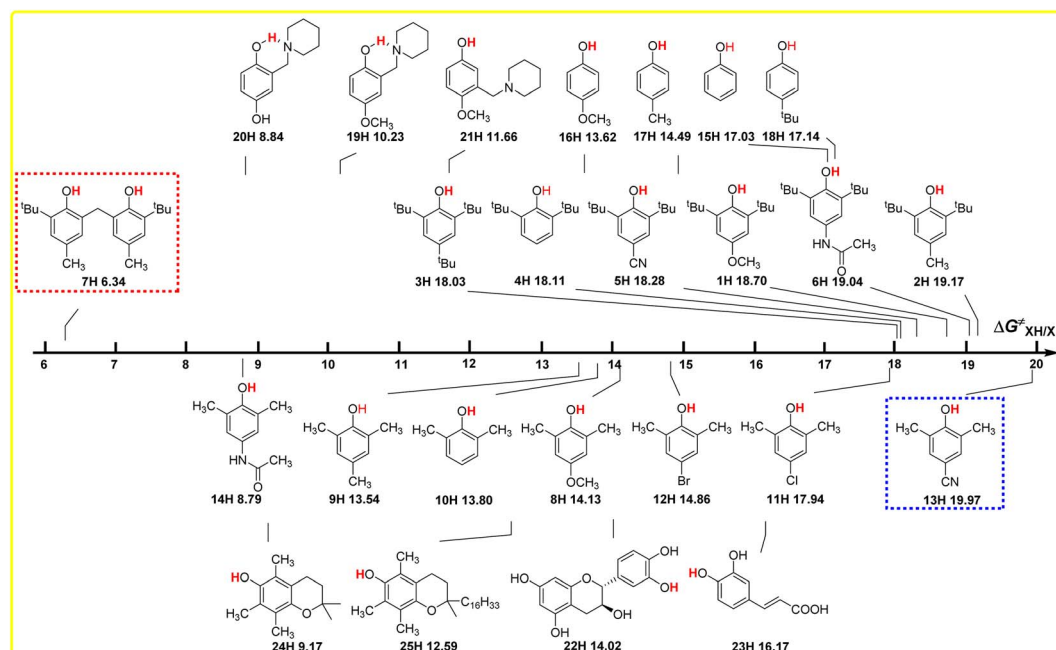
energy of the O–H bond in phenol, the electronic effects of substituent at position 4 on $\Delta G^\circ(\text{XH})$ of different phenol series are not uniform.

Similarly, by comparing the two series of 2,6-disubstituted-4-methoxyphenol and 2,6-disubstituted-4-methylphenol, it can be seen that the $\Delta\Delta G^\circ$ values obtained by the substitution of positions 2 and 6 with CH_3 and $t\text{Bu}$ are not the same in these two series. For different structures of 2,6-disubstituted phenols, the $\Delta\Delta G^\circ$ values caused by the substitution of position 4 from CH_3 to OCH_3 are also different, as shown in Scheme 3. When there are groups in the *o*-position of phenol that can form intramolecular hydrogen bonds with the phenolic hydroxyl group, the $\Delta G^\circ(\text{XH})$ values decrease and are concentrated between 75–77 kcal mol^{-1} , such as 19H–20H and 22H–23H.

Kinetic H-donating abilities of phenols $\Delta G_{\text{XH/X}}^\ddagger$

The intrinsic resistance energies $\Delta G_{\text{XH/X}}^\ddagger$ of O–H bonds in phenols are the kinetic parameters and used to characterize the kinetic resistance caused by the steric effect of the compound itself, which can generally be used to evaluate the kinetic H-donating abilities of O–H bonds with different structures. The bigger the $\Delta G_{\text{XH/X}}^\ddagger$ value is, the weaker the kinetic H-donating ability of XH is. In order to discover the dependence of $\Delta G_{\text{XH/X}}^\ddagger$ on the structures of XH, the direct vision dependence of $\Delta G_{\text{XH/X}}^\ddagger$ on the structures of XH is shown in Scheme 4. From Scheme 4, it is clear that the $\Delta G_{\text{XH/X}}^\ddagger$ values of 25 XH in CH_3CN at 298 K range from 6.34 kcal mol^{-1} for 6,6'-methylenebis(2-(*tert*-butyl)-4-methylphenol) (7H) to 19.97 kcal mol^{-1} for 2,6-dimethyl-4-cyanophenol (13H), and the order of $\Delta G_{\text{XH/X}}^\ddagger$ is different from the order of $\Delta G^\circ(\text{XH})$.

From Scheme 4, it can be seen that the order of $\Delta G_{\text{XH/X}}^\ddagger$ is 2,6-di-*tert*-butylphenol series > 2,6-di-methylphenol series \approx 4-substituted phenols, as the steric effect of $t\text{Bu}$ is bigger than that of CH_3 . For the 2,6-di-*tert*-butylphenol series, the $\Delta G_{\text{XH/X}}^\ddagger$ values are concentrated between 18 and 19 kcal mol^{-1} , indicating that the steric hindrance of different substituents at position 4 have little influence on the reaction centre O–H. However, for 2,6-dimethylphenol series, the $\Delta G_{\text{XH/X}}^\ddagger$ values are scattered, ranging from 8.79 to 19.79 kcal mol^{-1} , indicating that the hindrance of different substituents at position 4 has great influence on the reaction centre. Compared with the 2,6-di-*tert*-butyl phenol series, the different phenomenon also shows that the steric effect of *tert*-butyl group is far greater than that of the methyl group, so the steric effect of other groups at position 4 can be basically ignored in 2,6-di-*tert*-butyl phenol series, while the steric effect of methyl group is not prominent compared with



Scheme 4 Visual comparison of $\Delta G_{\text{XH/X}}^\ddagger$ among the 25 phenols of O–H bonds in CH_3CN at 298 K, the unit is kcal mol^{-1} .



other groups, so the $\Delta G_{\text{XH}/\text{X}}^\ddagger$ values of 2,6-dimethyl phenol series are relatively dispersed.

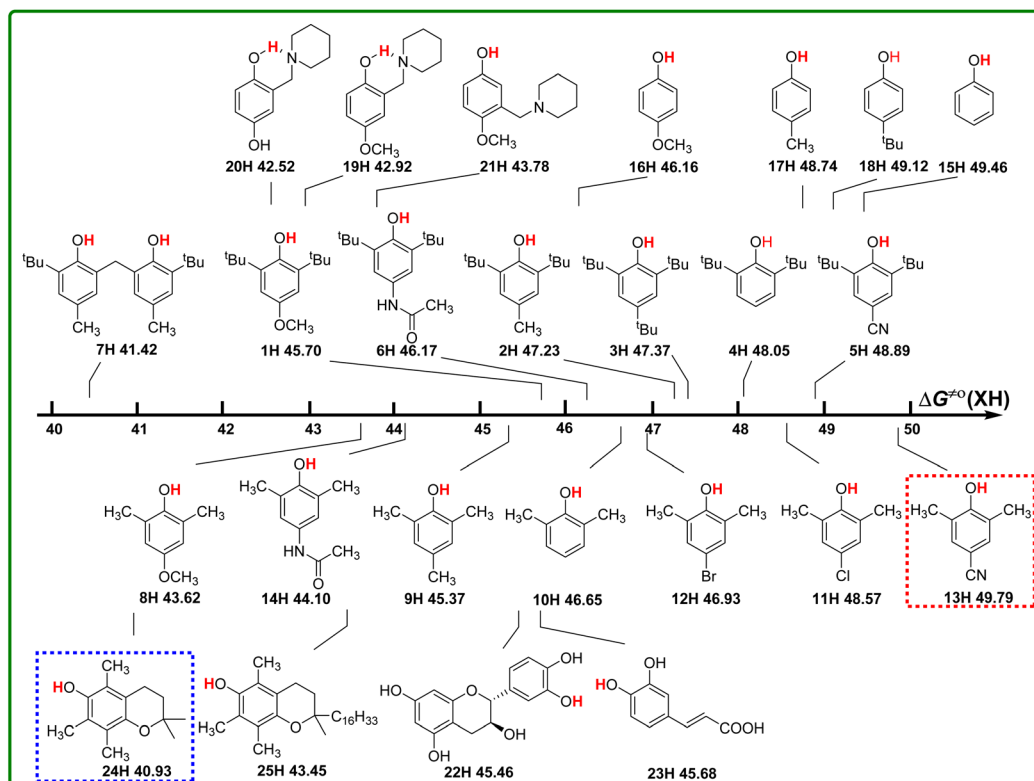
For 6,6'-methylenebis(2-*tert*-butyl)-4-methylphenol (7H), apparently, the steric hindrance of the compound is large, but because there are two reaction sites in the compound, and the two benzene rings are connected by the methylene group, the actual steric hindrance of the reaction centre is not large, and its kinetic H-donating ability is the strongest among these phenols. Compared with PMC (24H), the steric effect of the long-chain alkyl group at the far end of the reaction centre in α -tocopherol (25H) leads to an increase in $\Delta G_{\text{XH}/\text{X}}^\ddagger$ by 3.42 kcal mol⁻¹. At the same time, it can be seen from Scheme 2 that this long-chain alkyl group increases the $\Delta G^\circ(\text{XH})$ value of O–H bond by 1.60 kcal mol⁻¹.

In addition to the method of determining the intrinsic resistance energy $\Delta G_{\text{XH}/\text{X}}^\ddagger$ mentioned in this paper, a dynamic nuclear magnetic method is also mentioned in the literature, which is obtained from $\Delta G_{\text{XH}/\text{X}}^\ddagger$ by measuring the reaction rate of the pseudo-self-exchange HAT reaction.³³ The self-exchange rate constant for ¹Bu₃PhOH was determined by studying the pseudo-self-exchange reaction of ¹Bu₃PhO' + 2,6-di-*tert*-butyl-4-methylphenol.^{33a} In Table 3, the $\Delta G_{\text{XH}/\text{X}}^\ddagger$ values determined by eqn (3) in this work and by pseudo-self-exchange HAT reaction 2,6-¹Bu₂-4-CH₃Ph/¹Bu₃PhO' using dynamic ¹H NMR are listed. There is a certain deviation (2.36 kcal mol⁻¹) between the $\Delta G_{\text{XH}/\text{X}}^\ddagger$ values measured by the two methods. The possible reasons may be that there is a deviation between the pseudo-self-exchange HAT reaction and the real self-exchange HAT

Table 3 Comparison of the $\Delta G_{\text{XH}/\text{X}}^\ddagger$ values determined in this work and literature

Self-exchange HAT reaction	$\Delta G_{\text{XH}/\text{X}}^\ddagger$ (kcal mol ⁻¹)
	18.03 ^a
	15.67 ^b

^a $\Delta G_{\text{XH}/\text{X}}^\ddagger$ value is calculated by eqn (3): $\Delta G^{\ddagger\circ}(\text{XH}) \equiv 1/2[\Delta G_{\text{XH}/\text{X}}^\ddagger + \Delta G^\circ(\text{XH})]$. ^b $\Delta G_{\text{XH}/\text{X}}^\ddagger$ value is determined by pseudo-self-exchange reaction 2,6-¹Bu₂-4-CH₃Ph/¹Bu₃PhO' in ref. 33a.



Scheme 5 Visual comparison of $\Delta G^{\ddagger\circ}(\text{XH})$ among the 25 phenols of O–H bonds in CH₃CN at 298 K, the unit is kcal mol⁻¹.



reaction. The $\Delta G_{\text{XH}/\text{X}}^{\ddagger}$ values of 2,6-di-*tert*-butylphenol substituted at position 4 obtained by this method are all equal, which cannot reflect the influence of the substituent at position 4 on the $\Delta G_{\text{XH}/\text{X}}^{\ddagger}$. There is also an error in the reaction rate measured by dynamic ^1H NMR. However, the $\Delta G_{\text{XH}/\text{X}}^{\ddagger}$ value determined by eqn (3) in this work was calculated by the cross-HAT reaction method. The accuracy of the reaction rate constant k_{H} ($\Delta G_{\text{XH}/\text{Y}}^{\ddagger}$) measurement and the accuracy of the bond dissociation free energy [$\Delta G^{\circ}(\text{XH})$] will affect the accuracy of the $\Delta G_{\text{XH}/\text{X}}^{\ddagger}$ value. All the above-mentioned factors may lead to a difference in the $\Delta G_{\text{XH}/\text{X}}^{\ddagger}$ values obtained by the two methods.

Actual H-donating activities of phenols $\Delta G^{\ddagger\circ}(\text{XH})$

According to the definition of thermo-kinetic parameter $\Delta G^{\ddagger\circ}(\text{XH})$ (eqn (3)), it consists of both the thermodynamic parameter $\Delta G^{\circ}(\text{XH})$ and the kinetic parameter $\Delta G_{\text{XH}}^{\ddagger}$. Therefore, it is a comprehensive parameter that can well characterize the H-donating activity of the compound in HAT reactions. The bigger the value of $\Delta G^{\ddagger\circ}(\text{XH})$ is, the weaker the actual H-donating activity of XH is. Considering the above-mentioned thermodynamic and kinetic analyses, the structure-activity relationship of thermo-kinetic parameters is shown in Scheme 5. The $\Delta G^{\ddagger\circ}(\text{XH})$ values range from 40.93 kcal mol $^{-1}$ for PMC (24H) to 49.79 kcal mol $^{-1}$ for 2,6-dimethyl-4-cyanophenol (13H). The scale of $\Delta G^{\ddagger\circ}(\text{XH})$ is 8.85 kcal mol $^{-1}$, from which it can be seen that the structures of phenols have a great influence on their actual H-donating activities.

From Scheme 5, the actual H-donating activities of 2,6-di-*tert*-butyl-4-substituted phenols and 2,6-dimethyl-4-substituted phenols are in the same orders for the substituent at 4 position.

Although phenols 20, 22, and 23 have two phenolic OH groups (see Scheme 6), the labeled OH groups will react first, because they have a smaller bond dissociation free energy $\Delta\Delta G^{\circ}(\text{XH})$ than that of the other OH groups. Therefore, we focus on the more reactive hydrogen atom of the molecule. The $\Delta G^{\circ}(\text{XH})$ values of phenolic OH groups in phenols 20, 22, and 23 are listed in the following Scheme 6, which were obtained by the iBonD HM method. After the departure of the target hydrogen atom, the phenol radical forms an intramolecular hydrogen

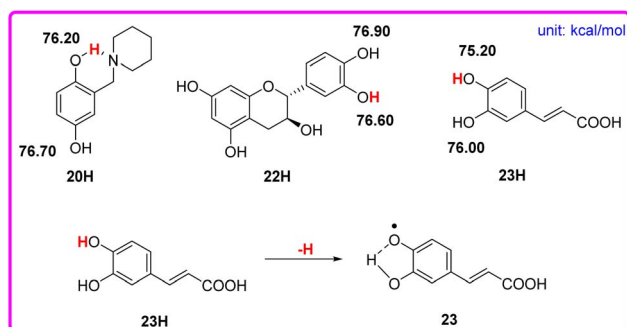
bond with the adjacent hydroxyl group or N atom. For example, phenol 23 is caffeic acid. After the target hydrogen atom leaves, the oxygen radical forms an intramolecular hydrogen bond with the adjacent OH groups, which stabilizes the radical to a certain extent, as shown in Scheme 6.

The thermo-kinetic parameter $\Delta G^{\ddagger\circ}(\text{XH})$ can be used not only to compare the H-donating activities of different phenols qualitatively and quantitatively, but also to provide data support for the accurate selection of appropriate antioxidants in scientific research and chemical production. Alkyl peroxy radicals (ROO^{\cdot}) such as CumOO $^{\cdot}$ [$\text{PhC}(\text{CH}_3)_2\text{OO}^{\cdot}$] are important oxygen-centred radicals that are involved in a variety of chemical and biological processes.¹⁹ In order to reduce the free radical CumOO $^{\cdot}$, we need to choose suitable antioxidants XH. In general, the selection of antioxidants should satisfy the following principles: first, the thermodynamic feasibility is satisfied; second, the rate constant of HAT reaction is easy to measure (k_2 's magnitude is among 10–10 5 M $^{-1}$ s $^{-1}$). As $\Delta G^{\circ}(\text{CumOO}^{\cdot}) = -81.90$ kcal mol $^{-1}$ and $\Delta G^{\ddagger\circ}(\text{CumOO}^{\cdot}) = -33.72$ kcal mol $^{-1}$ were available in our previous work,²² the value of $\Delta G^{\ddagger\circ}(\text{XH})$ for antioxidants should be within the scope of 44.35–49.80 kcal mol $^{-1}$. The calculation process is provided in ESI† according to eqn (2). Considering the thermodynamic feasibility and the rate constant of the HAT reaction, 2,6-di-*tert*-butyl-4-substituted phenols (1H–6H) and 2,6-dimethyl-4-substituted phenols (9H–13H) except for 4-CH $_3$ and 4-NHCOCH $_3$, (+)-catechin (22H) and caffeic acid (23H) can be selected as antioxidants for the reduction of CumOO $^{\cdot}$.

Actual H-abstraction activities of phenol radicals $\Delta G^{\ddagger\circ}(\text{X})$

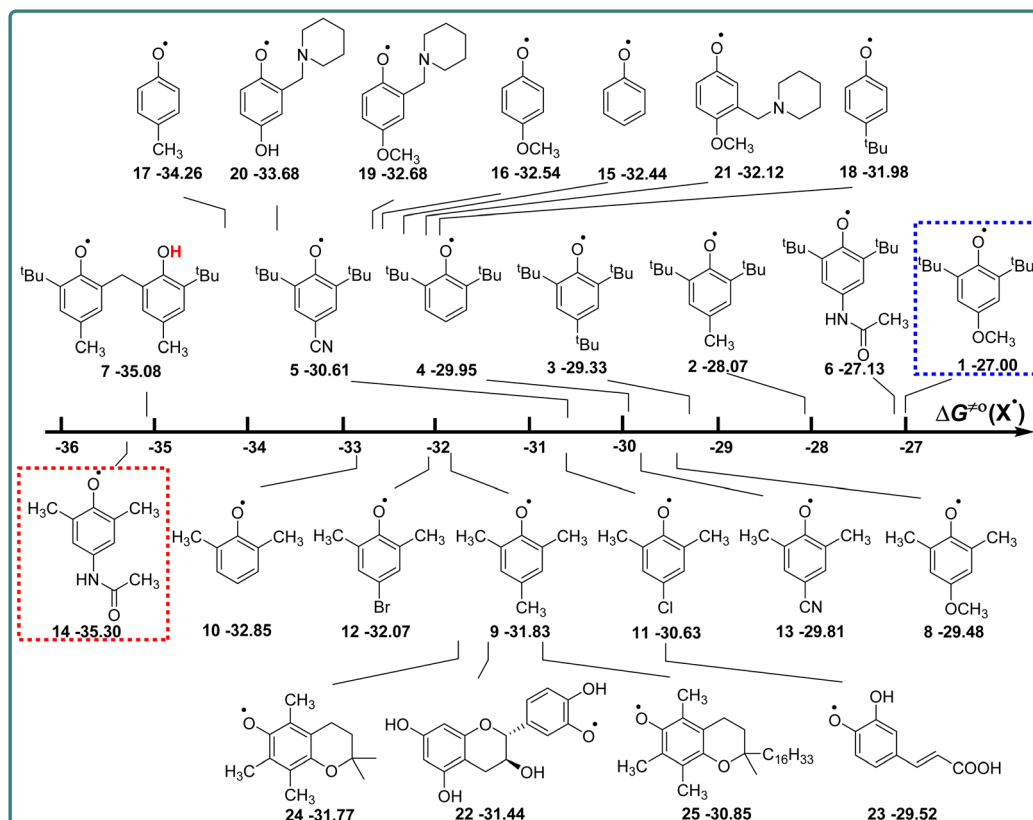
Phenols are not only one kind of H-donors, but also phenol radicals are important free radicals, which play an important role in the study of the kinetics and mechanism of the HAT reaction.^{14,15} In this part, the actual H-abstraction abilities of these phenol radicals are discussed using thermo-kinetic parameters $\Delta G^{\ddagger\circ}(\text{X})$ in detail. According to the definition of $\Delta G^{\ddagger\circ}(\text{X})$ (eqn (4)), $\Delta G^{\ddagger\circ}(\text{X})$ is composed of one half of the difference between $\Delta G_{\text{XH}/\text{X}}^{\ddagger}$ and $\Delta G^{\circ}(\text{XH})$, and the value is negative. The higher the negative value of $\Delta G^{\ddagger\circ}(\text{X})$ is, the stronger the oxidation ability of free radical X is, and the stronger the actual H-abstraction activity of X is. The visual comparison of $\Delta G^{\ddagger\circ}(\text{X})$ for these phenol radicals is shown in Scheme 7. The $\Delta G^{\ddagger\circ}(\text{X})$ values range from –27.00 kcal mol $^{-1}$ for 1 to –35.30 kcal mol $^{-1}$ for 14.

From Scheme 7, it can be observed that the H-abstraction activities $\Delta G^{\ddagger\circ}(\text{X})$ of X and the H-donating activities $\Delta G^{\ddagger\circ}(\text{XH})$ of XH are not in the same order. The phenol molecule has a strong H-donating activity, and its corresponding phenol radical may not have strong H-abstraction activity. For 2,6-di-*tert*-butyl-4-substituted phenols, the H-abstraction activities are in the order of CN > H > ^tBu > CH $_3$ > CH $_3$ CONH > OCH $_3$, which is in the opposite order of H-donating activities of XH. However, for 2,6-dimethyl-4-substituted phenols, the order of H-abstraction activities of X and the order of H-donating activities of XH are no obvious pattern.



Scheme 6 Visual comparison of $\Delta G^{\circ}(\text{XH})$ among the three phenols of O–H bonds that have 2 phenolic OH groups in CH $_3$ CN at 298 K, and the effect of the structure of phenol 23 for the abstraction of H.





Scheme 7 Visual comparison of $\Delta G^{\ddagger}(X)$ among the 25 phenols of O–H bonds in CH_3CN at 298 K, the unit is kcal mol^{-1} .

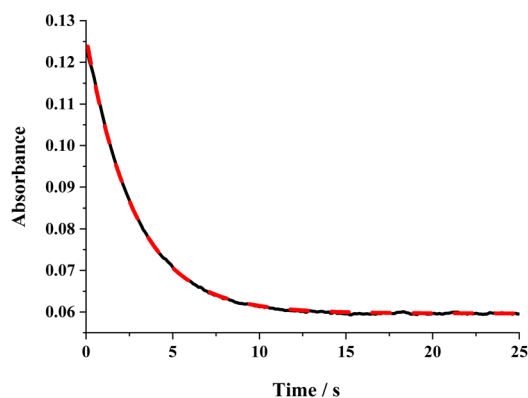


Fig. 1 Absorbance decay of ${}^t\text{Bu}_3\text{PhO}^\bullet$ (1.0 mM) in acetonitrile at $\lambda_{\text{max}} = 631 \text{ nm}$ following the addition of BNAH (20 mM) in deaerated anhydrous acetonitrile at 298 K (black line) and the fit (red line) using the pseudo-first-order kinetic model.

The $\Delta G^{\ddagger}(X)$ values of phenolic radicals are very important for the selection of free radicals and the judgment of reaction rate in HAT reactions. In our previous work, the thermo-kinetic parameter $\Delta G^{\ddagger}(\text{BNAH}) = 44.35 \text{ kcal mol}^{-1}$ of BNAH, the nicotinamide coenzyme analogue (NADH), has been obtained.²⁶ In this work, $\Delta G^{\ddagger}({}^t\text{Bu}_3\text{PhO}^\bullet) = -29.33 \text{ kcal mol}^{-1}$ was obtained. According to eqn (2), as long as $\Delta G^{\ddagger}(\text{BNAH})$ and $\Delta G^{\ddagger}({}^t\text{Bu}_3\text{PhO}^\bullet)$ are available, the activation free energy $\Delta G^{\ddagger}_{\text{BNAH}/{}^t\text{Bu}_3\text{PhO}^\bullet}$ of the HAT reaction between BNAH and ${}^t\text{Bu}_3\text{PhO}^\bullet$ can be evaluated. The $\Delta G^{\ddagger}_{\text{BNAH}/{}^t\text{Bu}_3\text{PhO}^\bullet}$ value is $44.35 - 29.33 = 15.02 \text{ kcal mol}^{-1}$. In order to verify the accuracy of the thermo-kinetic parameters obtained in this paper and verify the accuracy of the prediction of the HAT reaction rate by using the thermo-kinetic parameters, the HAT reaction between BNAH and ${}^t\text{Bu}_3\text{PhO}^\bullet$ was studied by a kinetic method. The absorbance decay of ${}^t\text{Bu}_3\text{PhO}^\bullet$ (1.0 mM) in acetonitrile at $\Delta\lambda_{\text{max}} = 631 \text{ nm}$

Table 4 Comparison of $\Delta G^{\ddagger}_{\text{calc.}}$ and $\Delta G^{\ddagger}_{\text{exp.}}$ of the HAT reaction BNAH/ ${}^t\text{Bu}_3\text{PhO}^\bullet$ in acetonitrile at 298 K

HAT reactions	ΔG^{\ddagger} (kcal mol^{-1})
	$\Delta G^{\ddagger}_{\text{calc.}} = 15.02 \text{ kcal mol}^{-1}$ $\Delta G^{\ddagger}_{\text{exp.}} = 14.79 \text{ kcal mol}^{-1}$ $\Delta\Delta G^{\ddagger} = 0.23 \text{ kcal mol}^{-1}$



following the addition of BNAH (20 mM) in deaerated anhydrous acetonitrile at 298 K (black line) and the fit (red line) using pseudo-first-order kinetic model is shown in Fig. 1. The comparison of the activation free energies $\Delta G_{\text{calc.}}^{\ddagger}$ and $\Delta G_{\text{exp.}}^{\ddagger}$ for the HAT reaction $\text{BNAH}/^t\text{Bu}_3\text{PhO}^\bullet$ and the difference between these two values [$\Delta\Delta G^{\ddagger} = \Delta G_{\text{calc.}}^{\ddagger} - \Delta G_{\text{exp.}}^{\ddagger}$] are listed in Table 4. The differences ($0.23 \text{ kcal mol}^{-1}$) between the experimental and the calculated values of the activation free energies $\Delta\Delta G^{\ddagger}$ are quite small.

Conclusions

In this article, the H-donating abilities of 25 well-known phenols and the H-abstraction abilities of the corresponding phenol radicals have been studied by using the bond dissociation free energy $\Delta G^\circ(\text{XH})$, kinetic intrinsic resistance energy $\Delta G_{\text{XH/X}}^{\ddagger}$ and thermo-kinetic parameters $\Delta G^{\ddagger\circ}(\text{XH})$ and $\Delta G^{\ddagger\circ}(\text{X})$ in thermodynamics, kinetics and actual HAT reactions. The $\Delta G^\circ(\text{XH})$ values have been determined by the iBonD HM method. The $\Delta G_{\text{XH/X}}^{\ddagger}$, $\Delta G^{\ddagger\circ}(\text{XH})$ and $\Delta G^{\ddagger\circ}(\text{X})$ values of phenols and phenol radicals in acetonitrile at 298 K have been determined according to eqn (2)–(4). The following conclusions could be drawn:

(1) The order of $\Delta G^\circ(\text{XH})$ of three types of phenols is 2,6-di-*tert*-butylphenol series > 2,6-di-methylphenol series > 4-substituted phenols. The presence of a substituent at position 4 has different effects on $\Delta G^\circ(\text{XH})$ of 2,6-di-*tert*-butylphenol, 2,6-dimethyl phenol and 4-substituted phenol series. The bond dissociation free energy changes $\Delta\Delta G^\circ$ caused by substituent change at position 4 are also different.

(2) If the group steric effect at positions 2 and 6 of phenol is large (as ^tBu), $\Delta G_{\text{XH/X}}^{\ddagger}$ of phenol in the HAT reaction mainly depends on the group at positions 2 and 6, and the steric effect at position 4 has a small effect on $\Delta G_{\text{XH/X}}^{\ddagger}$; however, if the steric effect at position 2 and 6 is not significant (as CH₃), the hindrance at position 4 has a large effect on $\Delta G_{\text{XH/X}}^{\ddagger}$. The differences between the method of determining $\Delta G_{\text{XH/X}}^{\ddagger}$ mentioned in this paper and the dynamic nuclear magnetic method mentioned in the literature are compared.

(3) The actual H-donating and H-abstraction activities of phenols and phenol radicals are compared using $\Delta G^{\ddagger\circ}(\text{XH})$ and $\Delta G^{\ddagger\circ}(\text{X})$. The accuracy of $\Delta G^{\ddagger\circ}$ and the accuracy of the prediction of the HAT reaction rate by using $\Delta G^{\ddagger\circ}$ are verified.

These parameters not only provide data support for the selection of antioxidants and free radicals in scientific research and practical production, but also provide new ideas for the design and synthesis of more efficient antioxidants and free radicals.

Experiment section

Kinetic measurements

The kinetics of the HAT reactions were conveniently monitored using an Applied Photophysics SX.18MV-R stopped-flow, which were thermostated at 298 K under strict anaerobic conditions in dry acetonitrile. The method of the kinetic measurement was a pseudo-first-order method. The concentration of the

antioxidant was maintained at more than 20-fold excess of the oxidant to attain the pseudo-first-order condition. The second-order rate constants (k_2) were derived from the plots of the pseudo-first-order rate constants *versus* the concentrations of the excessive reactants. In each case, it was confirmed that the rate constants derived from three to five independent measurements agreed within an experimental error of $\pm 5\%$.

Thermodynamic measurements

The bond dissociation free energies $\Delta G^\circ(\text{XH})$ are determined by the iBonD HM prediction methods: light GBM and SPOC descriptors with RMSE = 1.82, $r^2 = 0.980$ and mean absolute errors (MAEs) = 1.03 (95 : 5 train test split).^{28,29}

Conflicts of interest

The authors declare no competing financial interests.

Acknowledgements

Financial support from PhD Research Startup Foundation of Anyang Institute of Technology (BSJ2019032).

References

- (a) K. Murakami, S. Yamada, T. Kaneda and K. Itami, *Chem. Rev.*, 2017, **117**, 9302–9332; (b) L. Valgimigli and D. A. Pratt, *Acc. Chem. Res.*, 2015, **48**, 966–975; (c) K. U. Ingold and D. A. Pratt, *Chem. Rev.*, 2014, **114**, 9022–9046.
- (a) N. Holmberg-Douglas and D. A. Nicewicz, *Chem. Rev.*, 2022, **122**, 1925–2016; (b) Y. Qin, L. Zhu and S. Luo, *Chem. Rev.*, 2017, **117**, 9433–9520.
- (a) Y. Shang, X. Li, Z. Li, L. Shen, J. Zhou, R. Hu and K. Chen, *J. Mol. Struct.*, 2022, **1260**, 132830–132836; (b) M. R. Antonijević, E. H. Avdović, D. M. Simijonović, Ž. B. Milanović, A. D. Amić and Z. S. Marković, *Int. J. Mol. Sci.*, 2022, **23**, 490–505.
- (a) S. Immanuel, R. Sivasubramanian, R. Gul and M. Ahmad Dar, *Chem.-Asian J.*, 2020, **15**, 4256–4270; (b) S. Zhang, J. Shi, Y. Chen, Q. Huo, W. Li, Y. Wu, Y. Sun, Y. Zhang, X. Wang and Z. Jiang, *ACS Catal.*, 2020, **10**, 4967–4972.
- (a) J.-D. Yang, B.-L. Chen and X.-Q. Zhu, *J. Phys. Chem. B*, 2018, **122**, 6888–6898; (b) X.-Q. Zhu, Y. Tan and C.-T. Cao, *J. Phys. Chem. B*, 2010, **114**, 2058–2075; (c) X.-Q. Zhu, J.-Y. Zhang and J.-P. Cheng, *J. Org. Chem.*, 2006, **71**, 7007–7015.
- (a) M. Salamone, M. Galeotti, E. Romero-Montalvo, J. A. v. Santen, B. D. Groff, J. M. Mayer, G. A. DiLabio and M. Bietti, *J. Am. Chem. Soc.*, 2021, **143**, 11759–11776; (b) M. Salamone, G. A. DiLabio and M. Bietti, *J. Org. Chem.*, 2012, **77**, 10479–10487; (c) M. Finn, R. Friedline, N. K. Suleman, C. J. Wohl and J. M. Tanko, *J. Am. Chem. Soc.*, 2004, **126**, 7578–7584.
- (a) M. Salamone and M. Bietti, *Acc. Chem. Res.*, 2015, **48**, 2895–2903; (b) M. Salamone, M. Milan, G. A. DiLabio and M. Bietti, *J. Org. Chem.*, 2014, **79**, 7179–7184.



- 8 Y.-H. Fu, Z. Wang, Y. Zhang, G.-B. Shen and X.-Q. Zhu, *ChemistrySelect*, 2022, **7**, e202202625.
- 9 (a) J. J. Warren, T. A. Tronic and J. M. Mayer, *Chem. Rev.*, 2010, **110**, 6961–7001; (b) R. Amorati, S. Menichetti, C. Viglianisib and M. C. Foti, *Chem. Commun.*, 2012, **48**, 11904–11906.
- 10 (a) A. Coniglio, C. Galli, P. Gentili and R. Vadal`a, *Org. Biomol. Chem.*, 2009, **7**, 155–160; (b) H. Zhang, Z. Shi, R. Bai, D. Wang, F. Cui, J. Zhang and T. J. Strathmann, *Environ. Sci. Technol.*, 2021, **55**, 7681–7689.
- 11 (a) M. Salamone, R. Amorati, S. Menichetti, C. Viglianisib and M. Bietti, *J. Org. Chem.*, 2014, **79**, 6196–6205; (b) M. Finn, R. Friedline, N. Suleman, C. J. Wohl and J. M. Tanko, *J. Am. Chem. Soc.*, 2004, **126**, 7578–7584.
- 12 (a) R. Amorati, S. Menichetti, C. Viglianisib and M. C. Foti, *Chem. Commun.*, 2012, **48**, 11904–11906; (b) M. C. Foti, R. Amorati, G. F. Pedulli, C. Daquino, D. A. Pratt and K. U. Ingold, *J. Org. Chem.*, 2010, **75**, 4434–4440; (c) M. C. Foti, C. Daquino, I. D. Mackie, G. A. DiLabio and K. U. Ingold, *J. Org. Chem.*, 2008, **73**, 9270–9282.
- 13 (a) V. W. Manner, T. F. Markle, J. H. Freudenthal, J. P. Roth and J. M. Mayer, *Chem. Commun.*, 2008, 256–258; (b) S. C. Remke, T. H. Burgin, L. Ludvikova, D. Heger, O. S. Wenger, U. Gunten and S. Canonica, *Water Res.*, 2022, **213**, 118095–118107.
- 14 J. J. Warren and J. M. Mayer, *J. Am. Chem. Soc.*, 2008, **130**, 7546–7547.
- 15 C. D'Alfonso, M. Bietti, G. A. DiLabio, O. Lanzalunga and M. Salamone, *J. Org. Chem.*, 2013, **78**, 1026–1037.
- 16 M. Mazzonna, M. Bietti, G. A. DiLabio, O. Lanzalunga and M. Salamone, *J. Org. Chem.*, 2014, **79**, 5209–5218.
- 17 G. Litwinienko and K. U. Ingold, *J. Org. Chem.*, 2003, **68**, 3433–3438.
- 18 R. Amorati, S. Menichetti, C. Viglianisib and M. C. Foti, *Chem. Commun.*, 2012, **48**, 11904–11906.
- 19 L. Valgimigli, J. T. Banks, J. Luszyk and K. U. Ingold, *J. Org. Chem.*, 1999, **64**, 3381–3383.
- 20 Y.-H. Fu, G.-B. Shen, K. Wang and X.-Q. Zhu, *ChemistrySelect*, 2021, **6**, 8007–8010.
- 21 Y.-H. Fu, K. Wang, G.-B. Shen and X.-Q. Zhu, *J. Phys. Org. Chem.*, 2022, e4358.
- 22 Y.-H. Fu, G.-B. Shen, K. Wang and X.-Q. Zhu, *ACS Omega*, 2022, **7**, 25555–25564.
- 23 Y.-H. Fu, C. Geng, G.-B. Shen, K. Wang and X.-Q. Zhu, *ACS Omega*, 2022, **7**, 26416–26424.
- 24 Y.-H. Fu, Z. Wang, K. Wang, G.-B. Shen and X.-Q. Zhu, *RSC Adv.*, 2022, **12**, 27389–27395.
- 25 X.-Q. Zhu, F.-H. Deng, J.-D. Yang, X.-T. Li, Q. Chen, N.-P. Lei, F.-K. Meng, X.-P. Zhao, S.-H. Han, E.-J. Hao and Y.-Y. Mu, *Org. Biomol. Chem.*, 2013, **11**, 6071–6089.
- 26 Y.-H. Fu, G.-B. Shen, Y. Li, L. Yuan, J.-L. Li, L. Li, A.-K. Fu, J.-T. Chen, B.-L. Chen, L. Zhu and X.-Q. Zhu, *ChemistrySelect*, 2017, **2**, 904–925.
- 27 G. Litwinienko and K. U. Ingold, *J. Org. Chem.*, 2005, **70**, 8982–8990.
- 28 https://pka.luoszgroup.com/bde_prediction.
- 29 Q. Yang, Y. Li, J. D. Yang, Y. Liu, L. Zhang, S. Luo and J. P. Cheng, *Angew. Chem., Int. Ed.*, 2020, **59**, 19282–19291.
- 30 <https://ibond.nankai.edu.cn/>.
- 31 L. Konga, K. Donga, G. Lia, C. Yang, S. Lai and Y. Qu, *FirePhysChem*, 2022, **2**, 4–13.
- 32 X.-Q. Zhu, J. Zhou, C.-H. Wang, X.-T. Li and S. Jing, *J. Phys. Chem. B*, 2011, **115**(13), 3588–3603.
- 33 (a) J. J. Warren and J. M. Mayer, *Proc. Natl. Acad. Sci. U. S. A.*, 2010, **107**, 5282–5287; (b) A. Wu, E. A. Mader, A. Datta, D. A. Hrovat, W. T. Borden and J. M. Mayer, *J. Am. Chem. Soc.*, 2009, **131**, 11985–11997; (c) J. C. Yoder, J. P. Roth, E. M. Gussenhoven, A. S. Larsen and J. M. Mayer, *J. Am. Chem. Soc.*, 2003, **125**, 2629–2640.

